JOURNAL OF MATERIALS SCIENCE **34** (1999) 5133–5138

Macroscopic volume changes of PVF_2 undergoing uniaxial tension and creep

S. CASTAGNET, J. L. GACOUGNOLLE
Laboratoire de Mécanique et Physique des Matériaux (UMR 6617), Poitiers, France
P. DANG
CERDATO, Elf Atochem, Serquigny, France

Uniaxial tension and creep tests were performed on apolar cristalline PVF_2 at room temperature and above the high glassy transition temperature ($T_g = 40\,^\circ C$ and $T'_g = 60\,^\circ C$), for different strain-rates (tension) or applied stresses (creep). Volume changes were simultaneously measured to study cavitation damage occuring in this polymer when strained. Damage mechanisms were explicated. Influence of experimental conditions such as strain-rate or temperature was studied: onset of cavitation is delayed and volume changes more pronounced when molecular motions in amorphous phase are hindered, for lower temperature or higher strain-rates. This work brings elements for a better comprehension of PVF_2 global mechanical behaviour as damage is very linked to yield or creep studies.

1. Introduction

The most known form of damage in polymeric materials is crazing in glassy amorphous polymers: it was observed and formalized by many authors [1–7]. In semi-cristalline polymers [6–12], the great structure heterogeneity makes such studies more difficult. Most of the time, whitening occuring in damaged cristalline polymers is regarded as the macroscopical evidence of numerous microcracks (their faces can be linked or not by fibrillae).

In both amorphous and cristalline polymers, crazes or voids nucleate beneath defects or from areas exhibiting great density fluctuations. A large stress concentration factor and particularly a highly negative hydrostatic stress σ_h are necessary for voids formation; craze nucleation kinetics and saturation craze density increase with σ_h [1, 2, 13]. Two quite different mechanisms are responsible for craze propagation: fibrillae elongational creep and new polymer drawing from craze surfaces. It was shown that the later mechanism prevails over the former [1]. It can be easily understood that disentanglement is a crucial parameter in craze or void growth. For increasing stresses, fibrillae break inside the craze. Coalescence of resulting microcracks initiates fracture.

Most mechanical approaches dealing with polymers damage were based on volume change measurements during deformation. Tests performed in these studies were made mostly at constant strain-rate or constant load, in tension or compression. Two types of methods were adopted: liquid dilatational volumetry or principal strains simultaneous measurements (see [5] for a review). In the later case, both optical and 2 or 3-gauges apparatus were used. Volume change experiments were mostly developed for studying toughened polymers deformation mechanisms: shear, cavitation (inside particles or not) or debonding [11, 14–16]. As only shear mechanism occurs at constant volume, it was possible to isolate it. To discriminate cavitation and debonding, additional microscopical observations were supplied.

In the present paper, homopolymer PVF_2 is studied in an apolar phase. The aim is to precise which damage mechanisms take place in this polymer and the part they play in total deformation.

2. Experimental

2.1. Materials

The studied PVF_2 from α was supplied by ELF-ATOCHEM (Kynar 1000HD®). The monomer involved in this thermoplastic is $-[CH_2-CF_2]-$. Its molecular weight distribution (measured by gel permeation chromatography) is $M_w \approx 150.000$ and $M_n \approx 80.000$ g/mol. It means a molecular chain is made up of 2350 monomers on average and is about 0.35 μm long.

The cristallinity ratio of this material, deduced from WAXS experiments, is 55%. Like many highly cristalline polymers (PolyEthylene (PE), PolyPropylene (PP)) PVF_2 is known to exhibit a double glass-transition ($T_g = -40\,^\circ C$; $T'_g = 60\,^\circ C$). This suggests the existence of two amorphous phases; free and constrained. Below the main glass-transition temperature T_g, the whole amorphous phase is glassy; between T_g and T'_g, only free amorphous phase is relaxed; above T'_g, both free and constrained amorphous phases are rubbery. Melt temperature is 170 °C.

Dumbbell specimens were machined from 4 mm extruded sheets with specifications ISO R527 (gauge length 60 mm), in the extrusion direction to avoid a possible orientation effect. After machining, sections were

grained and edges smoothed with several fine emery papers.

2.2. Tests

Several kinds of uniaxial tests were performed on this material. Tensile tests at constant crosshead speed were carried out at room temperature (between T_g and T_g') and 65 °C (above T_g') in an Instron Testing Machine. The crosshead speeds ranged from 1 up to 100 mm/min implying strain-rates nearly constant between 2.5×10^{-4} and 2.5×10^{-2} s^{-1}. Constant-load creep tests were carried out in tension at room temperature in the same machine. Finally, in order to investigate the nature of deformation processes all along tensile tests, two types of tensile cyclic tests were performed at 23 and 65 °C as well. During "continuous" tensile cyclic tests, the sample undergoes following loading/unloading stages till increasing strains. In order to emphasize cavities closure in unloaded specimens, an hour recovery was applied at the end of each unloading. Such experiments will be called "recovered" tensile cyclic tests.

To estimate the cavitation damage occuring in strained PVF_2, a tensile dilatometric method was used involving the double extensometric system illustrated in Fig. 1. Axial strain was measured using a classical strain gage extensometer and transverse strain using a laser scan micrometer. It is pointed out that only two of the three strains (ε_{axial}, ε_{width} and $\varepsilon_{thickness}$) were available at the same time. Nevertheless, once the isotropy of transverse strains ($\varepsilon_{width} = \varepsilon_{thickness}$) had been experimentally checked, it could be possible to calculate true stress σ_t and volume strain ε_{vol} from load F, axial and transverse strains.

$$\varepsilon_{vol} = \varepsilon_{axial} + 2\varepsilon_{width} \tag{1}$$

$$\sigma_t = \frac{F}{1_{width} 1_{thickness}} \tag{2}$$

Elastic and dilatational contributions to the overall volume strain were calculated assuming that elastic, deviatoric (shear) and dilatational (cavitation) strains are linearly additive and that shear flow occurs without volume change [17]. So:

$$\left(\frac{\Delta V}{V}\right)_{el} = \frac{\sigma_t}{E} \tag{3}$$

$$\left(\frac{\Delta V}{V}\right)_{dilat} = \left(\frac{\Delta V}{V}\right) - (1-2\nu)\frac{\sigma_t}{E}$$

$$= \varepsilon_{vol} - (1-2\nu)\frac{\sigma_t}{E} \tag{4}$$

2.3. Tests reliability and repeatability

The significance of the results presented further highly depends on the performance and trustworthyness of the experimental device. Although the apparatus accuracy was good (the laser scan micrometer has a 0.1 μm resolution), some experimental bias must be taken into account. The main problem is the following: as the laser scan micrometer is fixed on the moving crosshead, the section which width is measured does not remain the same along the test. The sample "passes before" the laser beam. Local variations of the cross-section width resulting from specimens preparation described in section 2.1 are less than 1% in the scanned area: they contribute to the global error or $\varepsilon_{transverse}$. Because of calculation, errors on transverse strain are made twice on true stress and volume strain.

More than five identical tests were performed at different temperatures and strain-rates to check repeatability. Results at 65 °C and 2.5×10^{-3} s^{-1} are presented in Fig. 2. It can be deduced from all these tests that repeatability is satisfying: the scatter is about ±2% on true stress and ±5% on volume strain.

3. Results and discussion

T_g and T_g' delimitate three behavior fields for PVF_2. Below T_g, the sample is brittle and breaks without whitening. Between T_g and T_g', its behaviour is called "semi-ductile": the specimen homogeneously whitens; necking occuring at about 30% of axial strain cannot propagate and ductile fracture occurs within the neck.

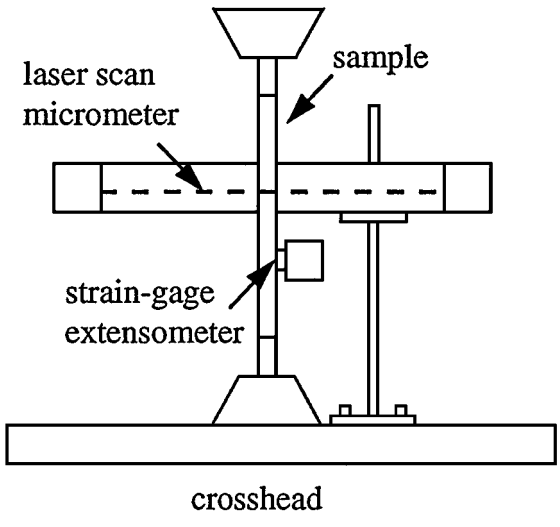

Figure 1 Experimental device.

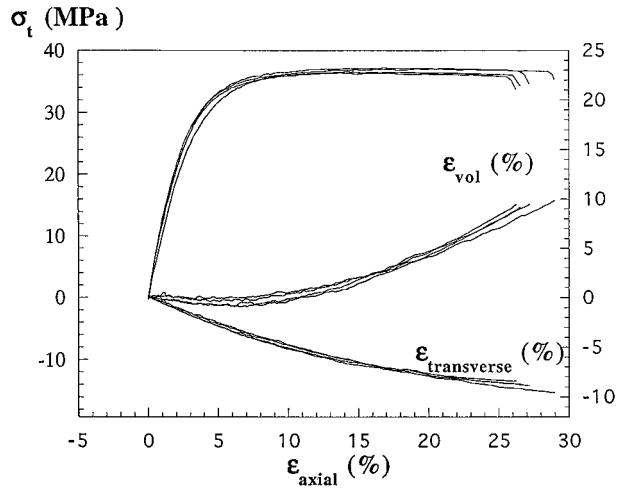

Figure 2 Repeatability of tensile tests (strain-rate: 2.5×10^{-3} s^{-1} and $T = 65$ °C).

Above T_g', the behaviour is classically ductile and necking propagates all along the sample. This whitening is regarded as the macroscopical evidence of micro-voids formation in the material. No colour change is observed below T_g: cavities are supposed then to form in rubbery amorphous phase. Results presented in this section are aimed to precise this cavitation damage phenomenon.

3.1. Damage mechanisms

An example of typical results from tensile tests is presented in Fig. 3: the evolutions of true stress, transverse strain and volume strain are plotted against axial stress. For axial strains below 2%, the deformation is mostly elastic without dilatational volume change. The onset of dilatation occurs for an axial strain equal to 5%. This critical strain corresponds to the whitening of the sample. Volume strain regularly increases up to 15% of axial strain. Then, the cross-section area nearly keeps a constant value and $\varepsilon_{vol} \approx 0.9\,\varepsilon_{axial}$: it can be deduced from formula (1) that voids mainly grow in the tensile direction. As illustrated in Fig. 4, damage phenomenon are similar but delayed during creep tests: the first strain stages occur without any volume change and dilatational mechanisms start when axial strain reaches about 7%.

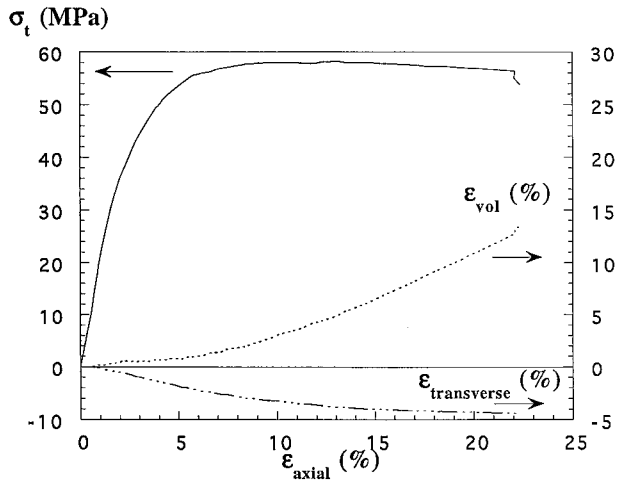

Figure 3 Tensile test (strain-rate: 2.5×10^{-3} s^{-1} and $T = 21\,^{\circ}$C).

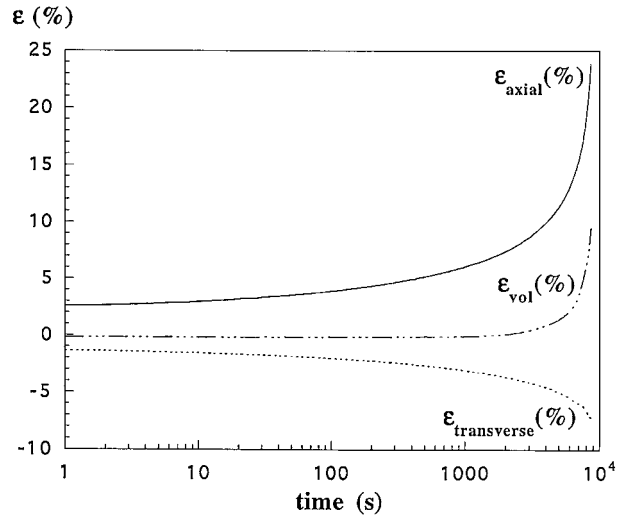

Figure 4 Creep test (applied load: 44 MPa and $T = 21\,^{\circ}$C).

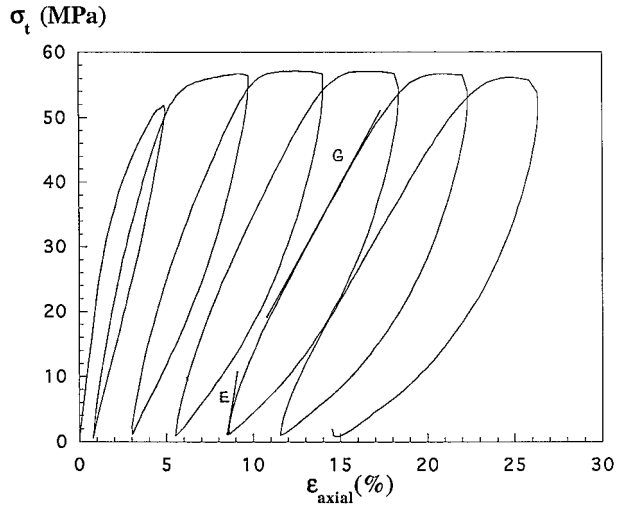

Figure 5 "Continuous" tensile cyclic test (strain-rate: 2.5×10^{-3} s^{-1} and $T = 21\,^{\circ}$C).

To precise the part of micro-voids in this thermoplastic deformation and understand how defects open and close, tensile cyclic tests must be analysed. Results from "continuous" tensile cyclic tests at room temperature are presented in Fig. 5. The loss of secant modulus which can be deduced from the σ-ε_{axial} curve (it decreases from 2400 MPa for the first cycle down to 640 MPa for the last one) asserts an increasing loss of cohesion in the material. Successive unloadings and loadings induce an increase of hysteresis areas: the strain mechanism becomes more and more dissipative. Last loadings exhibit two linear regimes: the first one governed by the Young modulus E, and the second one characterized by a second modulus G.

In this context, "recovered" tensile cyclic tests bring additional information because the recovery step setted to the unloaded sample accentuates micro-voids closure. Plots of true stress (a) and volume strain (b) against axial strain are presented in Fig. 6 at room temperature: different deformation regimes can be pointed out. At the beginning of unloading (stage A-B), stress strongly decreases from 58 down to 20 MPa whereas axial and volume strains slightly decrease (from 20 down to 18% for axial strain and from 8.5 down to 8% for volume strain). It can be attributed to the elastic contraction of cristallites and constrained amorphous phase. At the end of unloading (stage B-C), stress evoluates from 20 down to 0 MPa. In the same time, axial strain falls down from 18 to 9% and volume strain strongly decreases from 8 down to 5%: it can be attributed both to micro-voids closure and free amorphous phase recovery. Nevertheless, volume strain evolution (B-C) cannot be extrapolated to zero: micro-voids closure and amorphous phase recovery kinetics are different. At the end of unloading (point C), volume strain is not yet equal to zero: cavities are just partly closed. During recovery (stage C-D), volume strain follows a more pronounced decrease which can be extrapolated to zero (as indicated in dotted line in Fig. 6): kinetics of micro-voids closure and amorphous phase recovery are similar. Even if at the end of recovery, a residual volume strain remains, it is expected to become nil after a recovery step exceeding an hour or increasing temperature above T_g'.

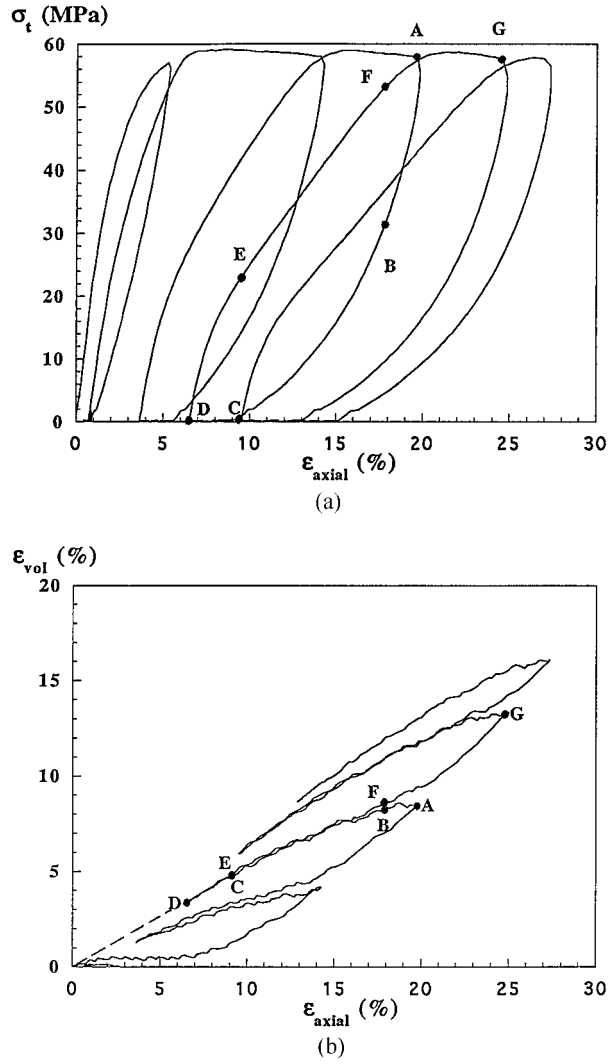

Figure 6 "Recovered" tensile cyclic test (strain-rate: 2.5×10^{-3} s^{-1} and $T = 21\,^{\circ}$C) (a) stress-strain curve (b) volume change.

At the beginning of next loading (stage D-E), the initial modulus is close to Young modulus, about 3000 MPa. Axial and volume strain increase are strictly identical to stage C-D: micro-voids strongly reopen, with the same kinetic as their closure during previous recovery. Stage E-F is the second linear regime observed in "continuous" tensile cyclic tests and characterized by modulus G. The end of this regime (point F) corresponds to point B. Evolutions of volume strain between E and F, and between B and C are identical: micro-voids go on opening in the same way as they closed during previous unloading. Finally, at the end of loading (stage F-G), damage increases and strongly accelerates in comparison with the previous cycle. This acceleration is much more emphasized when plastic flow regime is reached. It cannot be deduced, from our tests whether cavities already formed have grown or new voids have nucleated. As the later case is more energetically demanding, it can be supposed that previous micro-voids have grown.

Similar mechanical behaviour were observed in PolyOxyMethylene (POM) [12] and in PP [18]. Our results for PVF_2 confirm the interpretation of damage given for POM by Beguelin [12]. Similarities with rubbers behaviour above T_g (for instance the two modulus E and G) lead him to conclude that, above a critical axial strain, tie molecules formed a fibrillar structure between lamellae. Such a structure could be partly recoverable during unloading. During the following load, shear movements could be possible first between cristallites thanks to fibrils elasticity (stage D-E and E-F). Then, for increasing axial strain, disentanglement of fibrils would be responsible for the microvoids growth (stage F-G). Such cristalline mechanisms and fibrillar structures were observed in POM by Geil [19].

3.2. Viscoelasticity of the phenomenon

As pointed out in the previous section, damage mechanisms widely involve amorphous phase. They are expected so to be very sensitive to strain-rate and temperature. To check it, different strain-rates were applied to PVF2 at room temperature (similar results, not presented in this paper, were found at 65 °C) and different temperatures were considered at given strain-rates.

In Fig. 7, volume strains from tensile tests performed at 2.5×10^{-4}, 2.5×10^{-3} and 2.5×10^{-2} s^{-1} were plotted against axial strain. Only two decades were covered since very low strain-rates were not available in our tensile machine. No strain-rate influence on damage was observed in this range: ε_{vol}-ε_{axial} curves are identical; nucleation and growth stages occur similarly. In creep tests under high loads, a stationary creep regime is observed; strainrates are about 2×10^{-7} s^{-1}. So, to complete the strain-rates range, volume changes during these creep tests were compared to results obtained from tensile tests.

In Fig. 8, temperature influence was illustrated: volume strain was plotted vs. axial strain at 21 and 65 °C for two given strain-rates: 10 mm/min (2.5×10^{-3} strain-rate) (a) and 100 mm/min (2.5×10^{-2} strain-rate) (b).

Observations are identical for increasing temperature or decreasing strain-rate. First deformation stages are better accomodated and micro-voids nucleation is delayed. At room temperature and higher strain rates, cavitation begins at about 5% of axial strain. Increasing

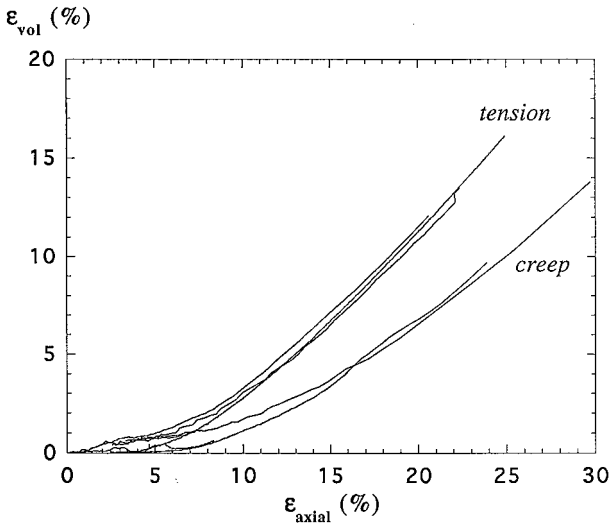

Figure 7 Strain-rate dependence of damage during tensile tests (strain-rates from 2.5×10^{-4} to 2.5×10^{-2} s^{-1} for tensile tests and about 2×10^{-7} s^{-1} for stationary creep).

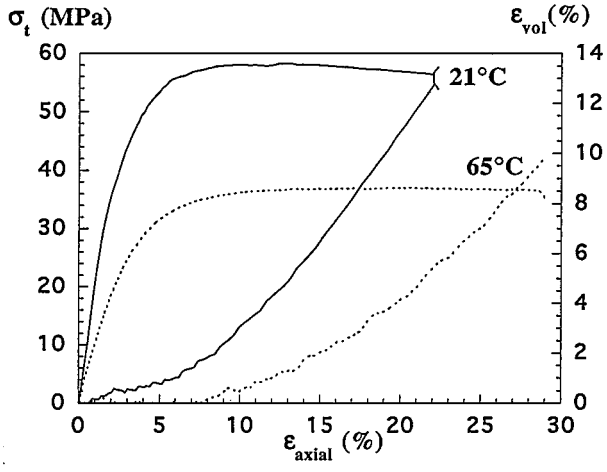

Figure 8 Temperature dependence of damage during tensile tests at 2.5×10^{-3} s^{-1} (a) and 2.5×10^{-2} s^{-1} (b).

temperature up to 65 °C, it only occurs at 8% of axial strain and decreasing strain rates (i.e. for creep tests), it is delayed to 7–8% of axial strain. Once damage process has started, the total amount of voids created at a given axial strain is clearly inferior for low strain-rates or high temperature. For instance in Fig. 8a, for an axial strain equal to 15%, volume strain is 6% at 21 °C and only 2% at 65 °C. This result is consistent with studies realized on PMMA and filled PP [5]. Nevertheless no additional information about temperature and strain-rate influences upon size and quantity of cavities can be brought from this macroscopical approach. Last observation involves damage evolution isotropy. Beyond axial strains about 15%, volume strain increases linearly to axial strain. At room temperature and higher strain-rates, $\varepsilon_{vol} \approx 0.9\,\varepsilon_{axial}$: this means that microvoids mainly grow in axial direction. At lower strain-rates (stationary creep), $\varepsilon_{vol} \approx 0.7\,\varepsilon_{axial}$ and increasing temperature up to 65 °C, this linear coefficient falls down to 0.6. It can be deduced that micro-voids no longer grow quasi exclusively in tensile direction.

The influence of both temperature and strain-rate cases on damage sensitivity can be explained by identical physical concepts. In PVF_2 deformation, cavitation damage and classical plastic flow appear like two competitive mechanisms which respective contributions depend on external conditions: cavitation is expected to begin in the material when relative molecular chains motions cannot accomodate deformation any more. Increasing temperature or decreasing strain-rate, chains motions in the relaxed part of amorphous phase are favoured. It explains the micro-voids nucleation occuring later, the global "created" volume decreasing and the damage developing in a more distributed way over 3D. This is clearly emphasized at temperatures above T_g' because not only free amorphous phase has an increased mobility: the whole amorphous phase including constrained part is relaxed.

3.3. Damage part in PVF_2 mechanical behaviour

As observed in PE for instance [21], PVF_2 exhibits a double yield. The first one occurs for axial strain between 5 and 10% depending on temperature and strain-rate; deformation remains homogeneous. The second one, occuring at axial strain around 30%, is necking.

Among yield criteria available for thermoplastics, maximum stress criterion is mostly used [22]. In our case, it is unable to discriminate first or second yield point since, according to the σ-ε curve shape, either first or second yield stress is the higher. Considere criterion is supported by instability concepts: yield is regarded as the critical point where antagonist phenomena of softening and strain-hardening equilibrate ($d\sigma/d\varepsilon = \sigma$) [23]. Table I gives values for yield strains (from Considere criterion) and cavitation onset strains (from the dilatational volume change beginning). It appears that damage part in PVF_2 yielding is very temperature dependant. At room temperature, only free amorphous phase is relaxed and cavitation, beginning before yielding, may be physically responsible for it. Above T_g', the whole amorphous phase is rubbery and accomodates deformation till yielding. In this last case, both damage and classical shear bands mechanisms contribute to PVF_2 yielding. It confirms the great sensitivity of damage to temperature emphasized in the previous section: the easier amorphous phase motions, the less micro-voids nucleation and growth are favoured.

It could be wondered whether Considere criterion—supported by instability concepts—was relevant for the first yield determination since deformation remains homogeneous. Links underlined here between damage and yielding assess its relevance: micro-voids nucleating all across the sample intrinsically represent physical instabilities, even if no cross section reduction is observed.

TABLE I Comparison between yielding and cavitation onset deformations

	$\varepsilon_{yielding}$ (%)	$\varepsilon_{cavitation}$ (%)
21 °C		
$\varepsilon' = 2.5 \times 10^{-4}$ s^{-1}	9	5.1
$\varepsilon' = 2.5 \times 10^{-3}$ s^{-1}	8.7	4.5
$\varepsilon' = 2.5 \times 10^{-2}$ s^{-1}	7.6	4
65 °C		
$\varepsilon' = 2.5 \times 10^{-3}$ s^{-1}	9.7	8.2
$\varepsilon' = 2.5 \times 10^{-2}$ s^{-1}	7	7.2

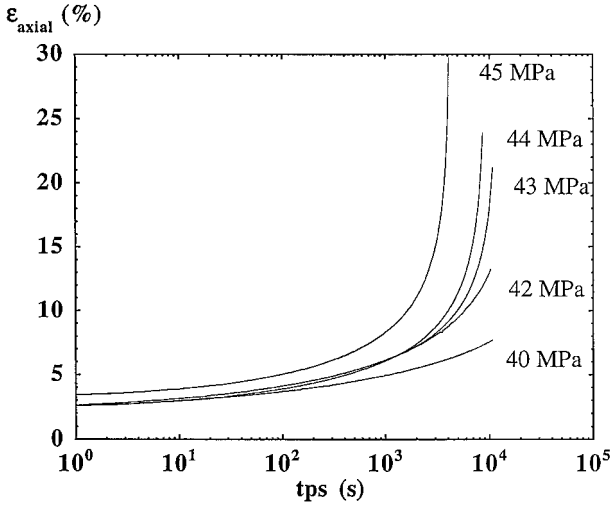

Figure 9 Creep tests at room temperature (21 °C).

Creep curves for applied stresses between 40 and 45 MPa at 21 °C are presented in Fig. 9 with corresponding volume strain evolutions. Several seconds are needed to reach the required high strengthes; consequently, first logarithmic creep is included in loading. Till axial strains of about 8% corresponding to the onset of cavitation, curves can be described by KWW laws. Beyond 8%, creep curves concern the damaged material: they are composed of a stationary creep step accelerating to tertiary creep at the end of the test. Such an evolution is close to phenomenon observed in metals creep experiments. Stationary creep would correspond to cavities nucleation and tertiary creep to cavities growing up and coalescence.

Activation volumes, calculated from tensile tests at 21 and 65 °C were found equal to 2600 and 2350 $Å^3$ respectively. These values are consistent with those usually found for this material [24]. Activation volume from creep tests at room temperature is 2300 $Å^3$: it is consistent with tensile tests results.

4. Conclusion

Through all unidirectional tests presented in this paper, mechanical evidence is brought of cavitational damage in PVF_2. It can be regarded as a competitive mechanism to classical shear yielding occuring when amorphous phase cannot accomodate deformation any more. Consequently, it is very sensitive to external conditions (strain-rate and temperature) as far as these parameters affect amorphous phase mobility. It is established that tensile and creep behaviours cannot be properly interpretated neglecting damage process. Cavitation appears so as a capital deformation mechanism to be taken into account to formulate PVF_2 mechanical behaviour laws.

References

1. E. J. KRAMER, in "Advances in Polymer Science," Vol. 52/53, edited by H. H. Kausch (Springer-Verlag, Berlin, 1983).
2. R. SCHIRRER, in "Introduction à la mécanique des polymères" (Apollor-INPL, France, 1995) p. 395.
3. A. J. KINLOCH and R. J. YOUNG, in "Fracture Behaviour of Polymers" (Elsevier Applied Science, London, 1983) p. 147.
4. J. G. WILLIAMS, in "Fracture Mechanics of Polymers" (Ellis Horwood Limited, New York, 1984) p. 123.
5. S. I. NAQUI and I. M. ROBINSON, *J. Mater. Sci* **28** (1993) 1421.
6. J. M. POWERS and R. M. CADDELL, *Polym. Eng. & Sci.* **12** (1972) 432.
7. P. P. BENHAM and D. McCAMMOND, *Plast. & Polym.* (1971) 130.
8. K. FRIEDRICH, in "Advances in Polymer Science," Vol. 52/53, edited by H. H. Kausch (Springer-Verlag, Berlin, 1983).
9. V. GAUCHER-MIRI, Thesis, Lille (France) 1995.
10. H. H. KAUSCH, C. J. G. PLUMMER and P. SCARAMUZZINO, in Proceedings of the 1st International Conference on Mechanics of Time-Dependant Materials (Ljubljiana) 1995.
11. C. B. BUCKNALL, P. S. HEATHER and A. LAZZERI, *J. Mater. Sci.* **16** (1989) 2255.
12. P. BEGUELIN, Thesis, EPF Lausanne, 1996.
13. K. CHO and A. N. GENT, *J. Mater. Sci.* **23** (1988) 141.
14. P. FRANCOIS, J. M. GLOAGUEN, B. HUE and J. M. LEFEBVRE, *J. Phys III* **4** (1994) 321.
15. S. Y. HOBBS and M. E. J. DEKKERS, *J. Mater. Sci.* **24** (1989) 1316.
16. M. E. J. DEKKERS and D. HEIKENS, *ibid.* **20** (1985) 3873.
17. D. HEIKENS, S. D. SJOERDSMA and W. J. COUMANS, *ibid.* **16** (1981) 429.
18. S. KREITMEIER, M. WITTKOP, T. WAGNER, D. GOTITZ and R. ZIETZ, *Colloid. Polym. Sci.* **273** (1995) 1008.
19. P. H. GEIL, in "Polymer Single Cristals" (John Whiley & Sons, New York, 1973).
20. D. C. YANG and E. L. THOMAS, *J. Mater. Sci. Lett.* **3** (1984) 929.
21. N. W. BROOKS, R. A. DUCKETT and I. M. WARD, *Polymer* **33** (1992) 1872.
22. S. HELLINCKS and J. C. BAUWENS, *Colloid. Polym. Sci.* **273** (1995) 219.
23. A. MOLINARI and C. G'SELL, in "Introduction à la mécanique des polymères" (Apollor-INPL, France, 1995) p. 321.
24. B. HARTMAN and G. F. LEE, *Polym. Eng. Sci.* **31** (1991) 231.

Received 28 July 1997
and accepted 24 February 1999